Journal of Nuclear Medicine, published on December 18, 2014 as doi:10.2967/jnumed.114.147603

^{18}F-FDG PET/CT Monitoring of β3 Agonist-Stimulated Brown Adipocyte Recruitment in White Adipose Tissue

(Short Running Head: FDG PET Monitors WAT Browning)

Jin-Won Park, Kyung-Ho Jung, Jin Hee Lee, Cung Hoa Thien Quach,

Seung-Hwan Moon, Young Seok Cho, Kyung-Han Lee

Department of Nuclear Medicine, Samsung Medical Center,

Sungkyunkwan University School of Medicine

Corresponding Author : Kyung-Han Lee, M.D

Department of Nuclear Medicine, Samsung Medical Center,

50 Ilwon-dong, Gangnam-gu, Seoul 135-710, Korea

Tel : 82-2-3410-2630; Fax : 82-2-3410-2639; khnm.lee@samsung.com

First Author: Jin-Won Park, M.S. (currently in training)

Department of Nuclear Medicine, Samsung Medical Center,

50 Ilwon-dong, Gangnam-gu, Seoul 135-710, Korea

Tel : 82-2-3410-2648; Fax : 82-2-3410-2639; jinwon.park@sbri.co.kr

This work was supported by Samsung Biomedical Research Institute Grant # SMX1131891.

ABSTRACT

There is rising interest in recruitment of brown adipocytes into white adipose tissue (WAT) as a means to augment energy expenditure for weight reduction. We thus investigated the potential of ^{18}F-FDG uptake as an imaging biomarker that can monitor the process of WAT browning. **Methods:** C57BL/6 mice were treated daily with the β3 agonist CL316,243, while controls received saline. ^{18}F-FDG micro-PET/CT was serially performed at 1 h after CL316,243 injection. Following sacrifice, interscapular brown adipose tissue (BAT) and WAT depots were extracted, weighed and measured for ^{18}F-FDG uptake. Tissues underwent immunostaining, and UCP1 content was quantified by Western blotting. **Results:** PET/CT showed very low ^{18}F-FDG uptake in both BAT and inguinal WAT at baseline. BAT uptake was substantially increased by a single stimulation with CL316,243. Uptake in inguinal WAT was only modestly elevated by the first stimulation, but uptake gradually increased to BAT level by prolonged stimulation. Ex-vivo measurements recapitulated the PET findings, and measured ^{18}F-FDG uptakes in other WAT depots were similar to inguinal WAT. WAT browning by prolonged stimulation was confirmed by a substantial increase of UPC1, COX4 and PRDM16 staining as markers brown adipocytes. UCP1 content, which served as a measure for extent of browning, was low in baseline inguinal WAT but linearly increased over 10 days of CL316,243 injection. Finally, image-based and ex vivo measured ^{18}F-FDG uptake in inguinal WAT correlated well with UCP1 content. **Conclusions:** ^{18}F-FDG PET/CT has the capacity to monitor brown adipocyte recruitment into WAT depots in vivo, and may thus be useful for screening the efficacy of strategies to promote WAT browning.

Key words: White adipose tissue, Brown adipose tissue, ^{18}F-FDG, PET, UCP-1, Beige cell

INTRODUCTION

Subcutaneous and visceral white adipose tissue (WAT) contributes to obesity by storing excess energy as intracellular lipid (*1,2*). By contrast, brown adipose tissue (BAT) can have a negative influence on weight gain by dissipating energy as heat (*3,4*). This thermoregulatory response is mediated through norepinephrine-activated β3 adrenergic receptor (β3AR) signaling. The exciting recent revelation that functional BAT is present not only in animals and young children but also in human adults (*5,6*) has fueled attempts to exploit its energy-consuming property to counter obesity (*7,8*). Unfortunately, however, obese patients have insufficient amounts of BAT, limiting the value of constitutive BAT for weight reduction (*9*).

On the other hand, obese subjects have abundant amounts WAT. It has recently become known that WAT can recruit clusters of adipocytes with brown-like phenotype. This process, called WAT browning, can be seen in mice stimulated by prolonged cold exposure or by β3AR agonists as a mimetic of cold stress (*10,11*). Brown-like cells recruited by WAT browning are referred to as 'beige' (pale brown) adipocytes (*12-14*). Based on these findings, there is rising interest on modulating the metabolic characteristics of WAT through beige cell recruitment to treat obesity. A particular attractiveness of this strategy is that it proposes to convert a fat-storing tissue into one that burns calories.

However, several questions need to be answered before targeting of WAT browning for weight reduction can be realized. For example, it is not known to what extent WAT can convert to beige cells or how various depots differ in this capacity. Furthermore, a method to evaluate the thermogenic impact of new drug candidates and allow a better understanding of the factors involved in optimal WAT browning is required. The current standard method for assessing WAT browning in animal models is based on invasive tissue sampling for histological or immunological detection of brown adipocyte-specific biomarkers, and the contribution of WAT browning on thermogenesis and systemic metabolism has relied on indirect inference from tissue characteristics.

As such, the ability to directly image energy consumption of WAT in living subjects may allow a better understanding of the mechanism of beige adipocyte recruitment and help facilitate the development of new candidate drugs. Visualization of heat radiation using infrared cameras is not a good measure of WAT thermogenesis due to dependence on thermal conductance, insulation and blood flow. Positron emission tomography-computed tomography (PET-CT) with ^{18}F-fluorodeoxyglucose (^{18}F-FDG) can readily image acutely activated brown adipocytes that have heightened glucose utilization for thermogenesis (*5,6)*. However, such studies to date have been mostly limited to acute BAT activation. Although β3AR stimulation has recently been shown to increase ^{18}F-FDG uptake in WAT of rodents (*15.16*), whether the level of ^{18}F-FDG uptake has sufficient accuracy to faithfully represent the magnitude of WAT browning has not been properly investigated. If ^{18}F-FDG can be shown to be a reliable biomarker, PET-CT imaging could help foster the in vivo translation of recent molecular discoveries related to WAT browning, and may provide insight on how obesity could be treated by modifying WAT metabolism. In this study, we thus investigated the ability of ^{18}F-FDG PET-CT to monitor and quantify recruitment of beige cells into WAT depots of living mice by prolonged simulation with the selective β3AR agonist CL316,243.

MATERIALS AND METHODS

Reagents and Cells

The β3 adrenoceptor agonist, CL316,243 was from Sigma-Aldrich. Normal goat serum, 3,3'-diaminobenzidine (DAB), chromogen solution, and citrate buffer were from Dako. Enhanced chemiluminescence kit was from Pierce, Rabbit polyclonal antibodies against glucose transporter 4 (GLUT4), uncoupling protein 1 (UCP1), and cytochrome c oxidase 4 (COX4) were from Abcam. Rabbit polyclonal antibody against PR domain containing 16 (PRDM16) was from Santa Cruz Biotech, rabbit monoclonal antibody against hexokinase-II was from Cell Signaling Technology, and HRP-labeled polymer conjugated antibody against rabbit IgG was from Dako. Wild-type male C57BL/6 mice (8 week; 21 g) were from Orient Bio.

Animal Preparation and CL316,243 Treatment

All animal experiments were in accordance with the National Institute of Health Guide for the Care and Use of Laboratory Animals and approved by the Institutional Animal Care and Use Committee. Mice were housed at a constant room temperature (RT) of 23°C with food and water given ad libitum, and were fed a standard diet that contains 62.1% carbohydrate, 24.7% protein, and 13.2% fat. Each morning, animals were intra-peritoneally injected with 1 mg/kg CL316,243 (n = 16) or saline (controls; n = 8). PET/CT imaging was serially performed at baseline (day -1) and on days 1, 4, 7, and 10 of treatment.

^{18}F-FDG Micro-PET/CT Acquisition and Image Analysis

Mice were fasted for 5 h prior to PET/CT studies. At 1 h after injection with CL316,243 or saline, animals were tail vein injected with 11.1 MBq of ^{18}F-FDG. Imaging was performed 1 h later under isoflurane anesthesia, using a micro-PET/CT scanner (Inveon; Siemens) without respiratory gating.

Acquisition of non-enhanced CT images was followed by emission PET imaging. Care was taken to maintain the mice in an environment of 23 to 25 °C.

On non-attenuation corrected tomographic PET/CT fusion images, polygonal regions of interest (ROIs) were drawn on interscapular BAT on sagittal slices, and inguinal WAT on coronal slices. Circular ROIs were placed in the left lung as background activity. From each ROI, mean standard uptake values (SUVs) and target-to-background (T/B) ratios were measured as indices of ^{18}F-FDG uptake.

Ex Vivo Quantification of ^{18}F-FDG Uptake in BAT and WAT Depots

Subsets of animals were sacrificed on day 1, 4, 7 or 10 (n = 4 each), immediately after PET/CT imaging. Inter-scapular BAT and WAT depots were extracted. Retroperitoneal and mesenteric WAT were from the abdominal cavity delimited by serous membranes divided into retroperitoneal and intraperitoneal areas. Epididymal WAT was from the abdomino-pelvic depot. Tissues were weighed and measured for ^{18}F-FDG activity on a high energy gamma counter (Parkin Elmer). Uptake levels were expressed as % of injection activity per gram of tissue (%IA/g). Tissues were fast-frozen until use for immune staining and western blots.

Immune Staining for Brown Adipocyte Markers

Tissues fixed in 4% paraformaldehyde were embedded in paraffin and microsectioned in 5 μm thickness. The sections were then deparaffinized in xylene and rehydrated in phosphate-buffered saline (PBS, pH 7.4). After heat-induced epitope retrieval with citrate buffer (pH 6.0) for 3 min at 121°C, endogenous peroxidase was blocked with 3% hydrogen peroxide in PBS for 10 min at RT. Sections treated with blocking solution for 20 min at RT to block nonspecific binding were were incubated with antibodies against UCP1 (1:100), PRDM16 (1:200), COX4 (1:200), GLUT-4 (1:400) or hexokinase-II (1:50) for 60 min at RT. PBS washed sections were incubated for 30 min at RT with HRP-conjugated antibodies against rabbit IgG. The color reaction was developed using DAB

substrate-chromogen solution, and sections were lightly counterstained with Mayer's hematoxylin before dehydration and mounting.

Quantitation of Brown Adipocytes by Mitochondrial UCP1 Content

Tissues minced in cold buffer containing 0.25 M sucrose and 5.0 mM N-Tris (hydroxlymethyl)methyl-2-amino ethanesulfonic acid buffer (pH 7.2) were homogenized in a Dounce homogenizer. After tissue debris removal, the supernatant was centrifuged at 10,000g for 10 min at 4°C. The mitochondrial pellet was re-suspended in buffer containing 20 mM Tris (pH 8.0), 1 mM EDTA, 100 mM NaCl, 0.9% sodium cholate, and 1% Triton X-100.

Mitochondria were lysed by incubation for 30 min on ice followed by freeze-thawing. Mitochondrial protein was separated by a 12% sodium dodecyl sulfate-polyacrylamide gel electrophoresis (SDS-PAGE), and transferred to a PVDF membrane. Following blocking, membranes were incubated overnight at 4°C with anti-UCP1 (1:1000) or anti-COX4 antibody (1:1000) in TBST (50 mM Tris, pH 7.5, 150 mM NaCl, 0.05% Tween-20) containing 5% skim milk. After washing three times for 10 min with TBST, the membrane was incubated with secondary antibodies for 1 h at RT. Immune reactive protein was detected with an enhanced chemiluminescence kit and measured for band densities.

Statistical Analysis

All data are shown as means ± SD. Comparison of values between multiple groups were performed by ANOVA with Tukey-Kramer post-hoc tests. Correlation was determined by linear regression analysis. P values < 0.05 were considered significant.

RESULTS

Acute Stimulation of Interscapular BAT ^{18}F-FDG Uptake

PET/CT images of interscapular fat showed no visible ^{18}F-FDG uptake at baseline, but a single dose of CL316,243 stimulated an acute and prominent enhancement of ^{18}F-FDG uptake and this finding recurred following each dose of CL316,243 for 10 days (Fig. 1A). Image analysis showed that T/B ratio of interscapular BAT was < 1 at baseline, but was markedly increased to 4.6 ± 1.2 only 1 h after the first CL316,243 dose (Fig. 1B). Interestingly, the ratio further increased on day 4 of CL316,243 injection. Image analysis using mean SUV showed nearly identical results with an increase from 0.7 ± 0.2 at baseline to 4.0 ± 1.3 at day 1, 5.6 ± 1.2 at day 4, 5.6 ± 1.8 at day 7, and 5.1 ± 3.0 at day 10. Ex vivo measurement of extracted tissue largely recapitulated the PET findings. Hence, ex vivo ^{18}F-FDG uptake was markedly increased from 2.1 ± 0.7 at baseline to 11.3 ± 2.5 %IA/gm by the first CL316,243 dose, and further increased to 25.6 ± 6.2 and 34.1 ± 5.7 %IA/gm on days 4 and 7, respectively. Uptake on day 10 (23.8 ± 11.5 %IA/gm) returned to a level comparable to that on day 7 (Fig. 1B).

Prolonged Stimulation Increases WAT ^{18}F-FDG Uptake

PET/CT images of inguinal WAT also showed no visible ^{18}F-FDG uptake at baseline or after saline injections (Fig. 2A). Unexpectedly, this tissue also demonstrated increased ^{18}F-FDG uptake by a single CL316,243 dose, although the magnitude was only modest compared to that of BAT. Stimulated uptake gradually became stronger with repeated CL316,243 doses (Fig. 2A). On image analysis, T/B ratio of inguinal WAT gradually increased from 0.4 ± 0.0 at baseline to 1.2 ± 0.2 on day 1, 2.3 ± 0.2 on day 4, and 2.6 ± 0.5 on day 7 (Fig. 2B). The ratio at day 10 day (2.2 ± 0.4) was similar to that at day 4. Again, mean SUV levels showed nearly identical results with an increase from 0.3 ± 0.0 at baseline to 1.1 ± 0.3 at day 1, 1.4 ± 0.3 at day 4, 1.7 ± 0.1 at day 7, and 1.5 ± 0.3 at day 10. Ex vivo measurements largely mirrored the PET image findings (Fig. 2B).

Epididymal and visceral WAT were evaluated by ex vivo measurements for ^{18}F-FDG uptake, and displayed temporal patterns of gradually increased uptake by prolonged stimulation similar to inguinal WAT (Supplement Fig. 1A). Uptake was greatest for mesenteric WAT, followed by retroperitoneal WAT, and lowest for epididymal WAT (15.3 ± 2.4, 12.3 ± 0.7, and 0.7 ± 0.3 %IA/gm at day 7, respectively). ^{18}F-FDG uptake of BAT and WAT are compared side by side in supplement figure 1B.

GLUT4 and Hexokinase-II Expression in Inguinal WAT

On identifying the mediator(s) for increased ^{18}F-FDG uptake in by β3AR stimulation, BAT displayed high expression of both Glut4 and hexokinase-II regardless of treatment (Fig.3). On the other hand, inguinal WAT showed low expression of both proteins at baseline. However, hexokinase-II expression was substantially increased after 10 days of stimulation, whereas GLUT4 expression was unaffected (Fig. 3).

Evidence for Brown Adipocyte Recruitment in Inguinal WAT

Inspection of hematoxylin and eosin stained tissue sections under a light microscope showed that interscapular BAT was filled with small brown adipocytes containing multiple small lipid droplets. In contrast, baseline inguinal WAT consisted of large round white adipocytes with a single massive lipid droplet. Following 10 days of CL316,243 injection, however, there was substantially increased numbers of cells with the brown adipocyte-like features (Fig. 3).

More compelling evidence of WAT browning was obtained by staining for UCP1, a thermogenic protein present exclusively in brown adipocytes. BAT showed intense UCP1 staining on abundant brown adipocytes regardless of treatment (Fig.4). Inguinal WAT showed very few UCP1 positive cells at baseline, which substantially increased following prolonged stimulation (Fig. 4). WAT browning was further evidenced by COX4 and PRDM16 staining. Again inguinal WAT showed very few positive cells at baseline, whereas the number of COX4 and PRDM16 stained cells significantly increased following prolonged stimulation (Fig. 5).

^{18}F-FDG Uptake in Stimulated WAT Correlates to UCP1 Expression

Quantitative analysis by western blotting of mitochondria protein confirmed high UCP1 expression level in BAT regardless of treatment, although there were further increases with repeated CL316,243 injection (Fig 6). Inguinal WAT showed undetectable levels of UCP1 level at baseline, but expression level steadily and significantly increased over 10 days of repeated stimulation (Fig 6). At day 10, UCP1 band intensity of WAT appeared similar to that of BAT, which indicates that equivalent amounts of mitochondrial protein, rather than that of fat tissue, have similar UCP1 content.

Finally, we evaluated whether ^{18}F-FDG uptake could serve as a surrogate marker of WAT browning as determined by UCP1 expression. As a result, regression analysis revealed good correlation of WAT UCP1 expression level to PET image-based ^{18}F-FDG uptake (Fig. 7A), as well as to ex vivo measured uptake level (Fig. 7B). In vivo and ex vivo measurements of ^{18}F-FDG uptake also showed a close correlation (Fig. 7C).

DISCUSSION

The results of this study show that ^{18}F-FDG uptake of interscapular BAT is prominently increased by a single challenge with CL316,243, which is consistent with acute metabolic responses previously observed in mice (*17,18*) and human subjects (*5,6*). Interscapular BAT thus served as a positive control in our study to investigate the ability of ^{18}F-FDG imaging to monitor beige cell recruitment into WAT.

Inguinal WAT displayed a relatively modest increase of ^{18}F-FDG uptake by the first CL316,243 dose, but uptake was gradually enhanced by repeated stimulations to finally reach a level comparable to that of the first-dose BAT response. Mirbolooki MR et al previously reported that WAT of rats show an increase of ^{18}F-FDG uptake by a single dose of CL 316243 (*15*). In addition, Quarta C et al. treated mice with CL316,2434 for 4 weeks and observed an increase of inguinal WAT ^{18}F-FDG uptake along with elevations of UCP-1 protein and PGC-1 mRNA expression (*16*). This finding suggests a link between enhanced FDG uptake and WAT browning as a result of prolonged β3 stimulation. Our study sought to further expand on these findings by a more detailed investigation to validate the potential of ^{18}F-FDG uptake as an imaging biomarker of WAT browning.

If ^{18}F-FDG uptake level reflects brown adipocyte recruitment, we would expect to observe a gradual increase of uptake over repeated stimulations. Therefore, we first longitudinally explored the time-course of how WAT ^{18}F-FDG uptake is enhanced during daily injections of CL316,243, a method previous shown to induce WAT browning over 10 days (*14*). Inguinal fat was selected for image analysis because it is better delineated by PET/CT, constitutes the biggest and physiologically most important WAT depot in mice, and is known to recruit beige adipocytes by adrenergic stimulation (*14,19*). On prolonged stimulation, inguinal WAT displayed only a modest increase of ^{18}F-FDG uptake by the first dose, but the magnitude of stimulated ^{18}F-FDG uptake gradually increased with repeat doses. By day 7, stimulated uptake became comparable to the first-dose BAT response. Of

the major determinants of glucose uptake, prolonged CL316,243 stimulation significantly increased inguinal WAT expression of hexokinase-II, but not Glut4.

As different WAT depots in mice are known to have unique biologic characteristics including adipocyte size, protein content and metabolic enzyme level (20), they could respond differently to browning stimulations. The beneficial effect of a drug would be limited if it induces browning only of inguinal WAT. We therefore evaluated whether the metabolic response of inguinal WAT monitored by ^{18}F-FDG uptake was representative of other major WAT depots. As a result, although retroperitoneal, mesenteric and epididymal WAT showed minor differences in ^{18}F-FDG uptake levels, all demonstrated a time-course of stimulated ^{18}F-FDG uptake that largely paralleled that of inguinal WAT. This suggests that WAT deposits from different sites may have similar roles in thermogenesis in response to prolonged β3 stimulation.

To qualify as a useful imaging biomarker, it is crucial that quantitative image results demonstrate a close correlation to the actual biologic effect-of-interest. We investigated this by comparing ^{18}F-FDG uptake levels to serial immunohistochemistry of brown adipocyte-specific makers as well as to UCP1 band intensities from western blots. Verification that metabolic response of inguinal WAT to prolonged stimulation was indeed related to browning was provided not only by visual inspection of morphologic changes but also by observing increased staining for UCP1, the most widely used brown adipocyte-specific marker. UCP1, a mitochondrial transmembrane protein that mediates ATP production-uncoupled transfer of protons from intermembrane space to mitochondrial matrix, is present exclusively in brown adipocytes (*3*,*4*). We further confirmed WAT browning by increased expression of 2 other major brown adipocyte markers, COX4 and RDM16. COX4 is a mitochondrial cytochrome-c oxidase abundantly present in brown adipocytes, and is a marker for oxidative phosphorylation-related gene expression (*21*). PRDM16 is a transcriptional complex that controls brown adipocyte formation (*22*), whose overexpression has been linked to beige cell induction and increased energy expenditure (*23*), supporting its critical role in WAT browning.

As a measure of the magnitude of WAT browning, we used UCP1 protein band intensities obtained from western blots. These data showed high baseline UCP1 expression in interscapular BAT, as expected. Daily CL316,243 injections further increased UCP1 levels, indicating an up-regulation of UCP1 density per mitochondria, which would account for the enhancement of stimulated ^{18}F-FDG uptake in interscapular BAT by repeated stimulation that we observed. Inguinal WAT showed undetectable levels of UCP1 at baseline, which raises the question of how ^{18}F-FDG uptake in this tissue was acutely increased, albeit modestly, by a single CL316,243 injection. Although white adipocytes do not express UCP1, they do express β3ARs. In mice knocked out of these receptors, agonist-induced thermogenesis is fully restored if the receptors are reinstalled in both BAT and WAT, but not BAT alone (*24*). Furthermore, mice lacking UCP1 were shown to retain a significant thermogenic response to β3AR stimulation (*25*). These findings suggest the possibility that white fat may elicit an acute metabolic response to β3AR stimulation in a manner independent of UCP1, although the precise mechanism remains to be revealed. With repeat CL316,243 doses, UCP1 protein began to appear in inguinal WAT by day 4, followed by a continued linear increase, finally reaching expression levels (per mitochondrial protein weight) comparable to that of BAT by day 10.

Finally, we found that UCP1 content closely correlated to image-based and ex vivo measured ^{18}F-FDG level before and during repeated β3AR stimulation. This indicates that ^{18}F-FDG PET/CT can detect the thermogenic response of recruited beige adipocytes, and may be able to estimate the extent of WAT browning by therapeutic agents. There was a relative decrease of WAT ^{18}F-FDG uptake at day 10 compared to day 7 that was divergent from the stronger UCP1 protein band intensity. Possible explanations may include a reduced sensitivity of UCP1 to repeated activation by CL316,2434, or a partial shift of stimulated energy expenditure from glucose to fatty acid as substrate. However, the precise cause for this finding is not clear and will require further investigation.

Although the relevance of beige cells in humans remains to be established, recent studies show that human fat tissue previously thought to be BAT actually contain islands of brown-like adipocytes

mixed within WAT, pointing to the presence of beige cells (*26*,*27*). Furthermore, in patients with retroperitoneal pheochromocytoma, abdominal visceral fat exposed to high noradrenaline concentrations for prolonged durations have shown intense ^{18}F-FDG uptake (*28*). These findings suggest that beige adipocytes could be of potential significance in human subjects as they are in mice.

CONCLUSION

Our results demonstrate that ^{18}F-FDG PET/CT has the capacity to monitor brown adipocyte recruitment into WAT depots in vivo. Imaging ^{18}F-FDG uptake may thus be useful for screening the efficacy of strategies to promote WAT browning, as well as help delineate its impact on energy expenditure by glucose utilization.

ACKNOWLEDGEMENTS

This work was supported by Samsung Biomedical Research Institute Grant # SMX1131891.

REFERENCES

1. Peirce V, Carobbio S, Vidal-Puig A. The different shades of fat. *Nature.* 2014;510:76-83.
2. Rosen ED, Spiegelman BM. Adipocytes as regulators of energy balance and glucose homeostasis. *Nature.* 2006;444:847-853.
3. Lowell BB, Spiegelman BM. Towards a molecular understanding of adaptive thermogenesis. *Nature.* 2000;404:652-660.
4. Harms M, Seale P. Brown and beige fat: development, function and therapeutic potential. *Nat Med.* 2013;19:1252-1263.
5. Van Marken Lichtenbelt WD, Vanhommerig JW, et al. Cold-activated brown adipose tissue in healthy men. *N Engl J Med.* 2009;360: 1500-1508.
6. Virtanen KA, Lidell ME, Orava J, et al. Functional brown adipose tissue in healthy adults. *N Engl J Med.* 2009; 360:1518-1525.
7. Tseng YH, Cypess AM, Kahn CR. Cellular bioenergetics as a target for obesity therapy. *Nat Rev Drug Discov.* 2010;9:465-482. .
8. Lidell ME, Enerback S. Brown adipose tissue - a new role in humans? *Nat Rev Endocrinol.* 2010;6: 319–325.
9. Ravussin E, Kozak LP. Have we entered the brown adipose tissue renaissance? *Obes Rev.* 2009;10:265-268.
10. Wu J, Cohen P, Spiegelman BM. Adaptive thermogenesis in adipocytes: Is beige the new brown? *Genes Dev.* 2013;27: 234-250.
11. Granneman JG, Li P, Zhu Z, Lu Y. Metabolic and cellular plasticity in white adipose tissue I: effects of β3-adrenergic receptor activation. *Am J Physiol. Endocrinol Metab.* 2005;289:E608-E616.
12. Wu J, Bostro¨m P, Sparks LM, et al. Beige adipocytes are a distinct type of thermogenic fat cell in mouse and human. *Cell.* 2012;150:366-376.

13. Rosenwald M, Perdikari A, Ru¨licke T, Wolfrum C. Bi-directional interconversion of brite and white adipocytes. *Nat Cell Biol.* 2013;15:659–667.

14. Vegiopoulos A, Müller-Decker K, Strzoda D, Schmitt I, et al. Cyclooxygenase-2 controls energy homeostasis in mice by de novo recruitment of brown adipocytes. *Science.* 2010;328:1158-1161.

15. Mirbolooki MR, Upadhyay SK, Constantinescu CC, Pan ML, Mukherjee J. Adrenergic pathway activation enhances brown adipose tissue metabolism: a [^{18}F]FDG PET/CT study in mice. *Nucl Med Biol.* 2014;41:10-16.

16. Quarta C, Lodi F, Mazza R, et al. (^{11})C-meta-hydroxyephedrine PET/CT imaging allows in vivo study of adaptive thermogenesis and white-to-brown fat conversion. *Mol Metab.* 2013;2:153-160.

17. Cypess AM, Doyle AN, Sass CA, et al. Quantification of human and rodent brown adipose tissue function using ^{99m}Tc-methoxyisobutylisonitrile SPECT/CT and ^{18}F-FDG PET/CT. *J Nucl Med.* 2013;54:1896-2901.

18. Mirbolooki MR, Constantinescu CC, Pan ML, Mukherjee J. Quantitative assessment of brown adipose tissue metabolic activity and volume using ^{18}F-FDG PET/CT and β3-adrenergic receptor activation. *EJNMMI Res.* 2011;1:30.

19. Waldén TB, Hansen IR, Timmons JA, Cannon B, Nedergaard J. Recruited vs. nonrecruited molecular signatures of brown, "brite," and white adipose tissues. *Am J Physiol Endocrinol Metab.* 2012; 302:E19-E31.

20. Sackmann-Sala L, Berryman DE, Munn RD, Lubbers ER, Kopchick JJ. Heterogeneity among white adipose tissue depots in male C57BL/6J mice. Obesity (Silver Spring). 2012;20:101-111.

21. Gburcik V, Cleasby ME, Timmons JA. Loss of neuronatin promotes "browning" of primary mouse adipocytes while reducing Glut1-mediated glucose disposal. *Am J Physiol Endocrinol Metab.* 2013;304:E885-894.

22. Seale P, Bjork B, Yang W, et al. PRDM16 controls a brown fat/skeletal muscle switch. *Nature.* 2008; 454: 961–967.
23. Ohno H, Shinoda K, Spiegelman BM, Kajimura S. PPARgamma agonists induce a white-to-brown fat conversion through stabilization of PRDM16 protein. *Cell Metab.* 2012;15:395-404.
24. Grujic D, Susulic VS, Harper ME, et al. Beta3-adrenergic receptors on white and brown adipocytes mediate beta3-selective agonist-induced effects on energy expenditure, insulin secretion, and food intake. A study using transgenic and gene knockout mice. *J Biol Chem* 1997;272: 17686-17693.
25. Granneman JG, Burnazi M, Zhu Z, Schwamb LA. White adipose tissue contributes to UCP1-independent thermogenesis. *Am J Physiol Endocrinol Metab* 2003;285: E1230–E1236.
26. Wu J, Boström P, Sparks LM, et al. Beige adipocytes are a distinct type of thermogenic fat cell in mouse and human. *Cell.* 2012;150:366-376.
27. Sharp L, Shinoda K, Ohno H, et al. Human BAT possesses molecular signatures that resemble beige/brite cells. *PLoS ONE.* 2012;7:e49452.
28. Dong A, Wang Y, Lu J, Zuo C. Hypermetabolic mesenteric brown adipose tissue on dual-time point FDG PET/CT in a patient with benign retroperitoneal pheochromocytoma. *Clin Nucl Med.* 2014;39:e229-e232.

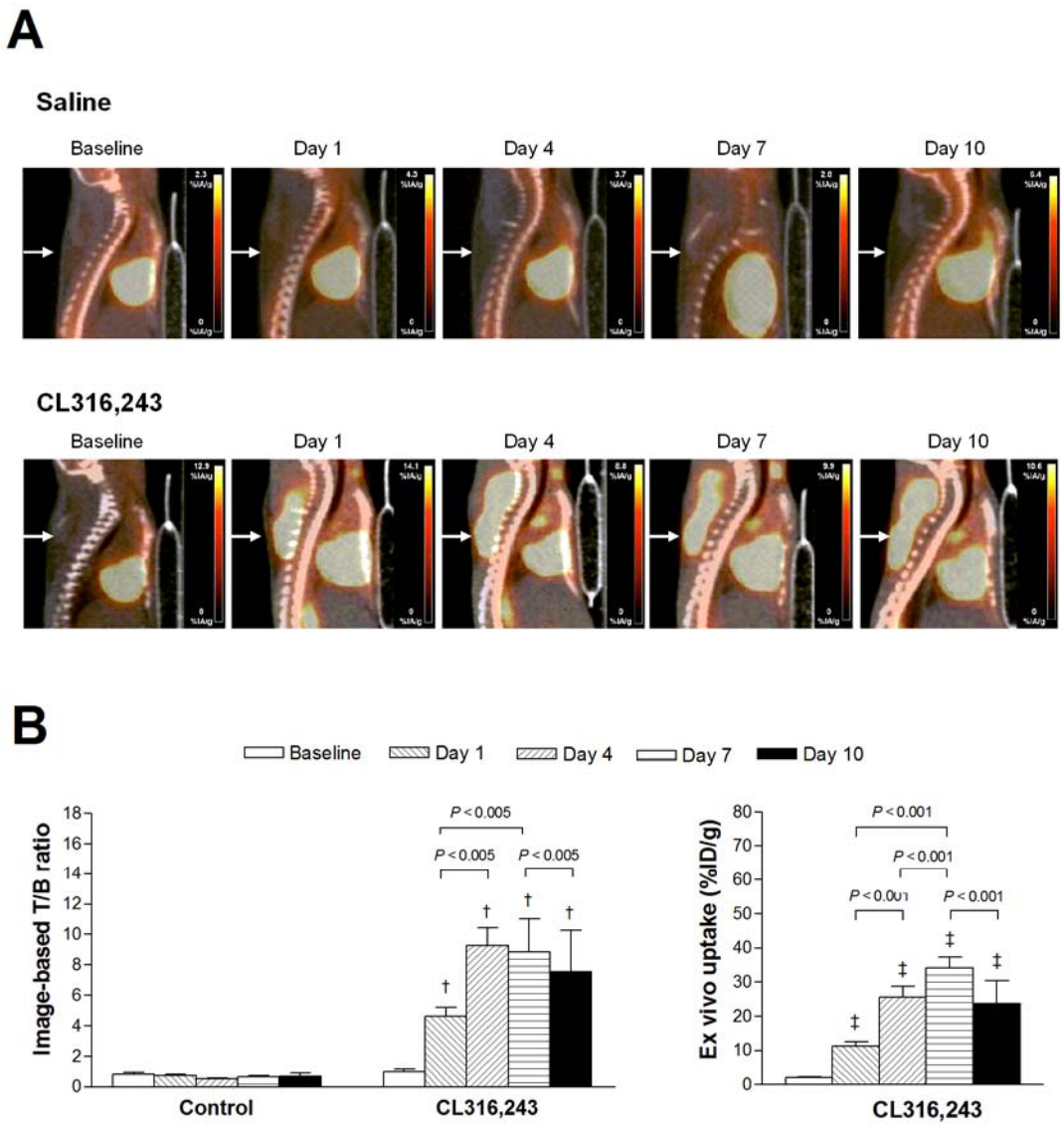

Figure 1. Interscapular BAT ^{18}F-FDG uptake by β3 adrenergic stimulation. (A) Sagittal ^{18}F-FDG PET/CT images of interscapular BAT (arrows) at baseline and during repeated saline or CL316,243 (1 mg/kg) injection. (B) Image-based target (T; interscapular BAT) to background (B; lung) count ratios from polygonal regions-of-interest (left), and ex vivo measured interscapular BAT uptake in % adminsteted-dose per gram-tissue (%IA/g; right). Bars are mean ± SD of values obtained from 3 or 4 animals per group. †P <0.005; ‡P <0.001, compared to baseline CL316,243 group.

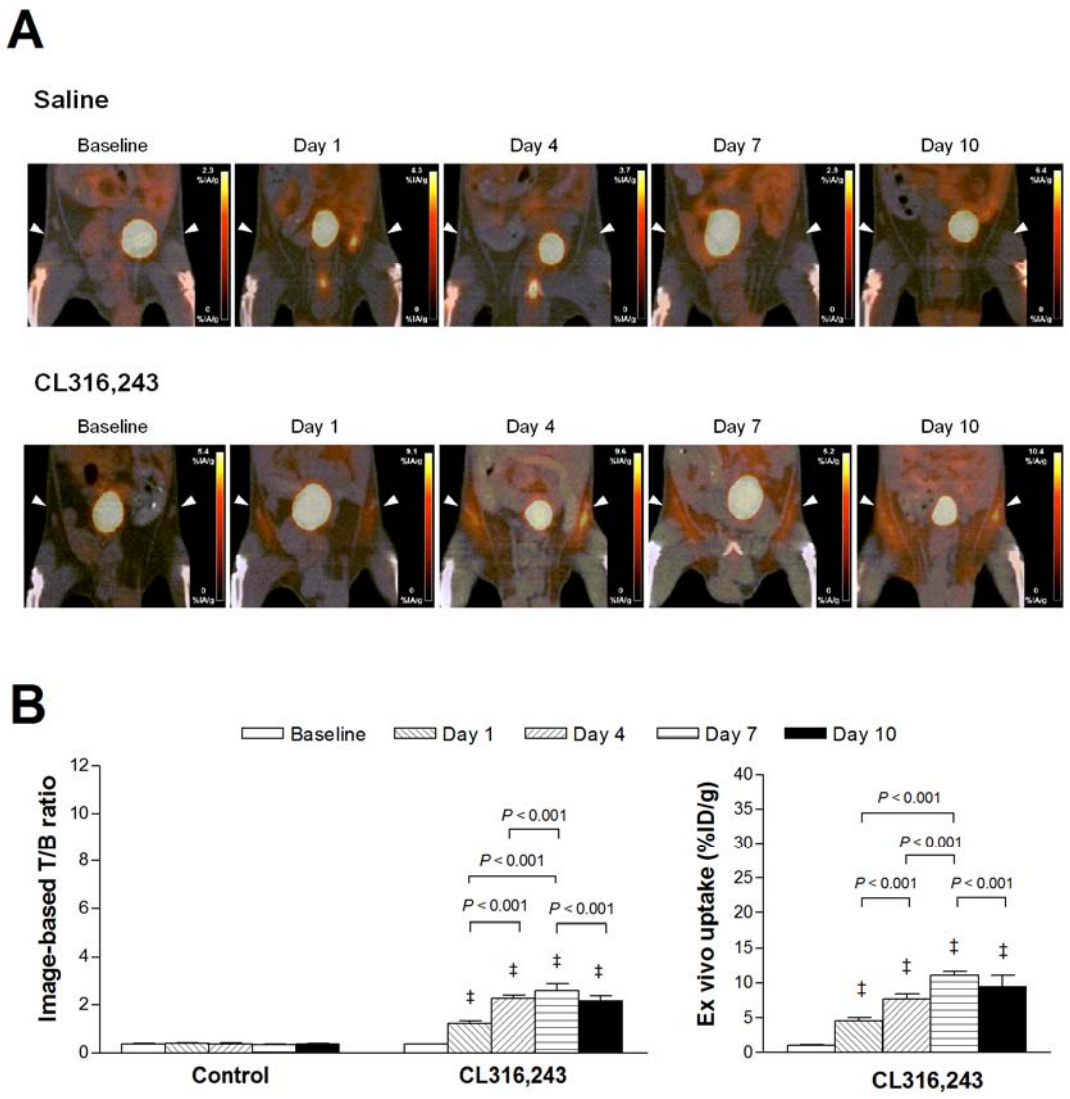

Figure 2. Inguinal WAT ^{18}F-FDG uptake by β3 adrenergic stimulation. (A) Coronal ^{18}F-FDG PET/CT images of inguinal WAT (arrowheads) at baseline and during repeated saline or CL316,243 (1 mg/kg) injection. (B) Image-based target (T; inguinal WAT) to background (B; lung) count ratios (left), and ex vivo measured inguinal WAT uptake (right). Bars are mean ± SD of values obtained from 3 or 4 animals per group. ‡P <0.001, compared to baseline CL316,243 group..

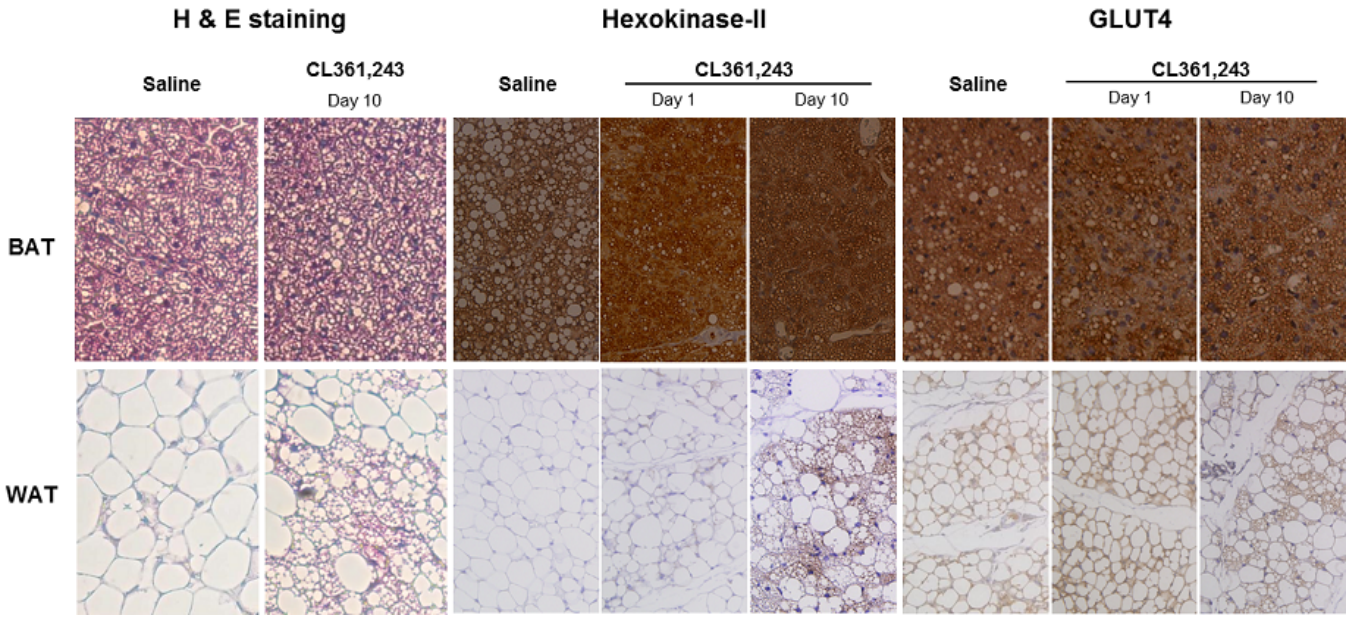

Figure 3. Hematoxylin and eosin staining, and immune-staining of hexokinase-II and GLUT4 expression. Interscapular BAT and inguinal WAT extracted at day 1 or 10 were paraffin embedded, microsectioned and immunostained. Magnification, x200 for hematoxylin and eosin staining and x100 for other staining

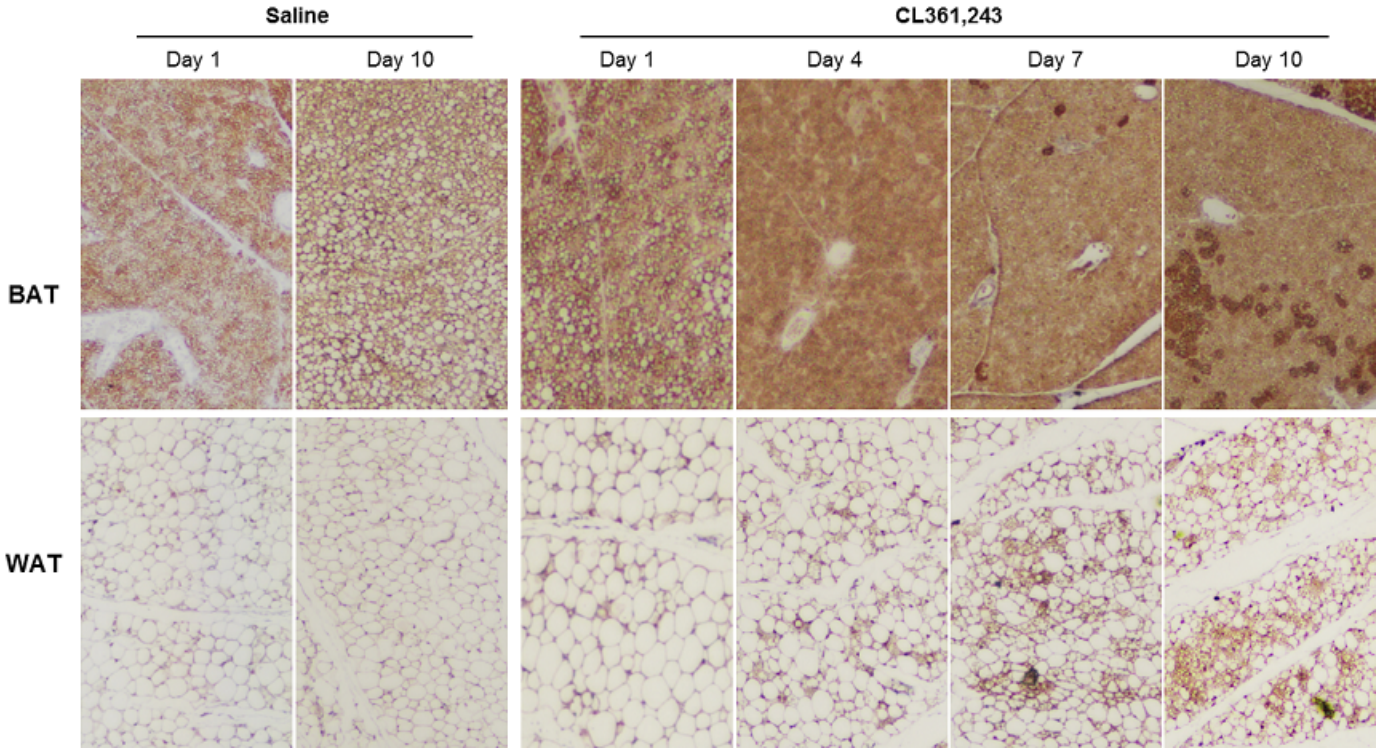

Figure 4. Immunostaining of UCP1 expression in interscapular BAT and inguinal WAT extracted at indicated time points. Magnification, x100

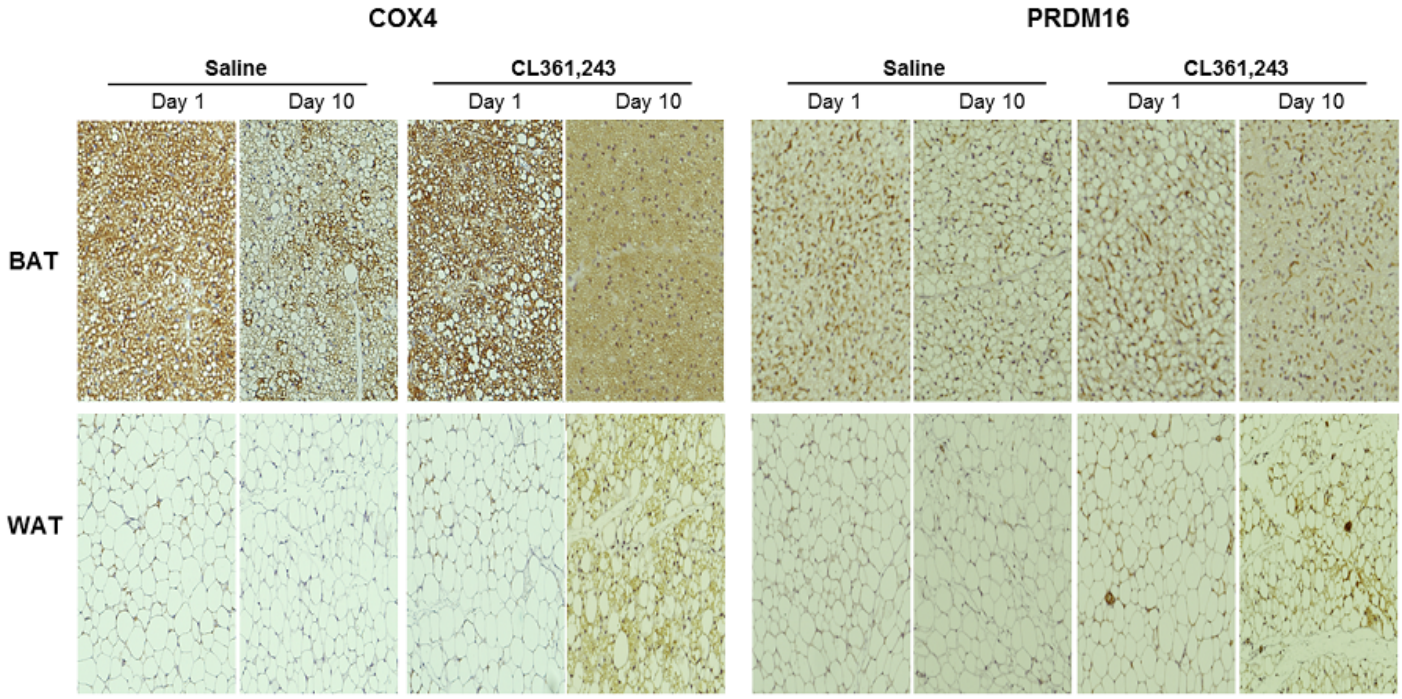

Figure 5. Immunostaining of COX5 and PRDM16 expression in interscapular BAT and inguinal WAT extracted at indicated time points. Magnification, x100

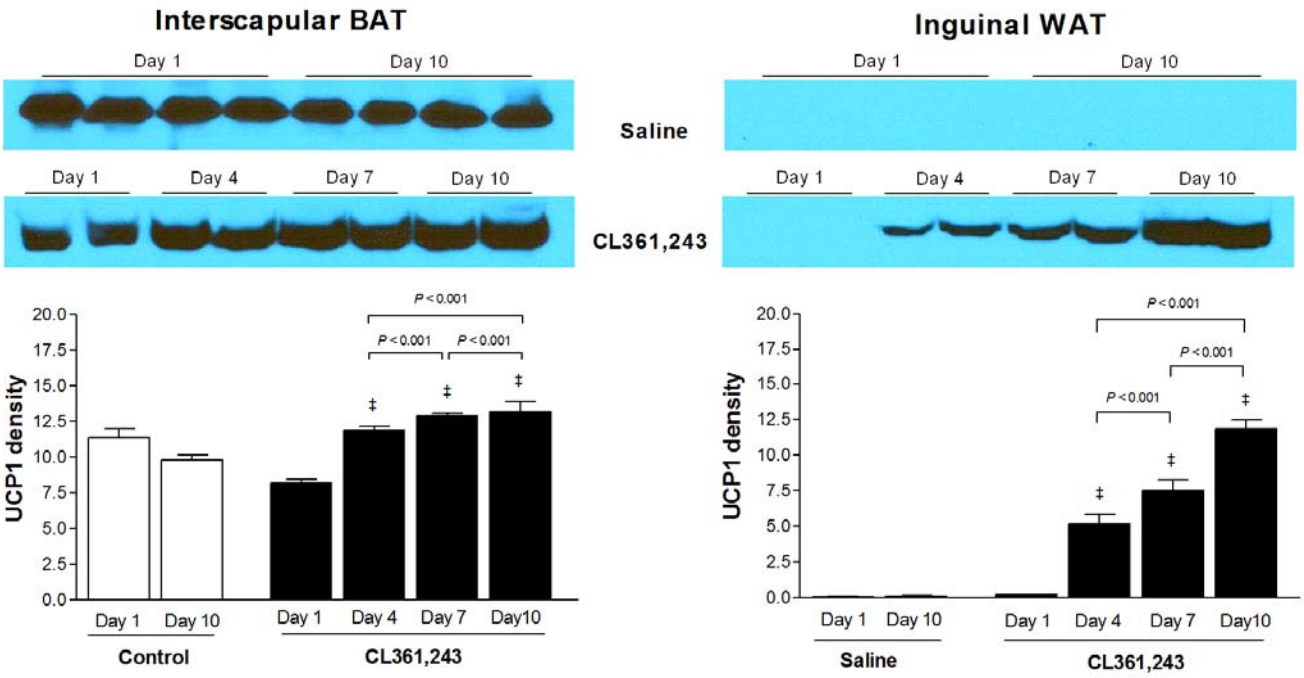

Figure 6. Quantitative measurement of UCP1 expression. UCP1western blots of mitochondrial protein from interscapular BAT and inguinal WAT (top) and quantified band densities (bottom). COX4 expression was used as loading control (not shown). Bars are mean ± SD of band density relative to that of COX4 obtained from 3 or 4 animals per group. ‡P<0.001, compared to CL316,243 group at day 1.

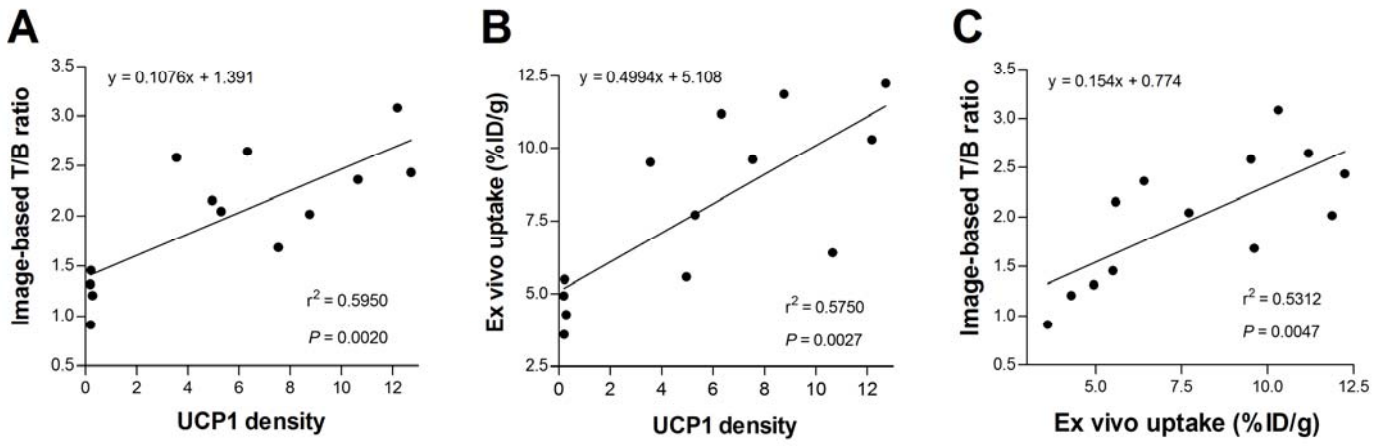

Figure 7. Correlation between ^{18}F-FDG uptake and UCP1 expression. (A,B) Linear regression analysis between inguinal WAT UCP1 level and image-based (A) and ex vivo measured ^{18}F-FDG uptakes (B). (C) Correlation between image-based and ex vivo measured ^{18}F-FDG uptake. Data points are from mice treated with CL316,243 for 1 (n = 4), 4 (n = 3), 7 (n = 3), or 10 days (n = 3).